

Assessment of dosimetric impact of interfractional 6D setup error in tongue cancer treated with IMRT and VMAT using daily kV-CBCT

Prashantkumar Shinde¹, Anand Jadhav², V. Shankar³, Sanjay J. Dhoble¹

¹Department of Physics, Rashtrasant Tukadoji Maharaj Nagpur University, Nagpur, India

²Department of Radiation Oncology, Sir H N Reliance Foundation Hospital and Research Centre, Mumbai, India

³Department of Radiation Oncology, Apollo Cancer Center, Chennai, India

ABSTRACT

Background: This study aimed to evaluate the dosimetric influence of 6-dimensional (6D) interfractional setup error in tongue cancer treated with intensity-modulated radiation therapy (IMRT) and volumetric modulated arc therapy (VMAT) using daily kilovoltage cone-beam computed tomography (kV-CBCT).

Materials and methods: This retrospective study included 20 tongue cancer patients treated with IMRT (10), VMAT (10), and daily kV-CBCT image guidance. Interfraction 6D setup errors along the lateral, longitudinal, vertical, pitch, roll, and yaw axes were evaluated for 600 CBCTs. Structures in the planning CT were deformed to the CBCT using deformable registration. For each fraction, a reference CBCT structure set with no rotation error was created. The treatment plan was recalculated on the CBCTs with the rotation error (R_{Error}), translation error (T_{Error}), and translation plus rotation error ($T+R_{Error}$). For targets and organs at risk (OARs), the dosimetric impacts of R_{Error} , T_{Error} , and $T+R_{Error}$ were evaluated without and with moderate correction of setup errors.

Results: The maximum dose variation ΔD (%) for $D_{98\%}$ in clinical target volumes (CTV): CTV-60, CTV-54, planning target volumes (PTV): PTV-60, and PTV-54 was -1.2%, -1.9%, -12.0%, and -12.3%, respectively, in the $T+R_{Error}$ without setup error correction. The maximum ΔD (%) for $D_{98\%}$ in CTV-60, CTV-54, PTV-60, and PTV-54 was -1.0%, -1.7%, -9.2%, and -9.5%, respectively, in the $T+R_{Error}$ with moderate setup error correction. The dosimetric impact of interfractional 6D setup errors was statistically significant ($p < 0.05$) for $D_{98\%}$ in CTV-60, CTV-54, PTV-60, and PTV-54.

Conclusions: The uncorrected interfractional 6D setup errors could significantly impact the delivered dose to targets and OARs in tongue cancer. That emphasized the importance of daily 6D setup error correction in IMRT and VMAT.

Key words: dosimetric impact; interfractional 6D setup error; kV-CBCT; tongue cancer; head and neck cancer; IMRT; VMAT

Rep Pract Oncol Radiother 2023;28(2):224-240

Introduction

Tongue cancer is one of the most common human papilloma virus (HPV)-attributed head and neck malignant tumors globally [1]. Modern, state-of-the-art

radiation therapy techniques, such as intensity modulated radiation therapy (IMRT) and volumetric modulated arc therapy (VMAT), play a vital role in managing head and neck cancer. Both IMRT and VMAT deliver precise and highly conformal

Address for correspondence: Prashantkumar Shinde, M.Sc., D.R.P., Department of Physics, Rashtrasant Tukadoji Maharaj Nagpur University, Amravati Road, Nagpur 440033, India, tel: (+91) 9923472316; e-mail: pk.shinde16@gmail.com

This article is available in open access under Creative Common Attribution-Non-Commercial-No Derivatives 4.0 International (CC BY-NC-ND 4.0) license, allowing to download articles and share them with others as long as they credit the authors and the publisher, but without permission to change them in any way or use them commercially

doses to the targets while sparing the surrounding organs at risk (OARs) [2–3]. A multicentric randomized trial found that IMRT and VMAT had better tumor control and lower toxicity than 2D and 3D RT techniques, which was corroborated by two subsequent meta-analyses and dosimetric investigations [4–6]. For IMRT and VMAT, the highly conformal dose distribution to the target with rapid dose falloff outside the target perimeter needs extreme precision in target localization to get the optimal benefit [7, 8]. 3D image guidance techniques used in IMRT and VMAT allow for greater precision in the intended dose delivery [8–13]. Even with the rigid immobilization, target localization and setup error persist and could have an adverse dosimetric effects [14–16]. The magnitudes of interfractional setup errors in head and neck cancer are significant [13, 17–21]. They have substantial dosimetric effects on delivered doses to targets and OARs. Previous studies found that interfractional translational and rotational errors significantly alter the delivered dose to target volumes and OARs [22–31]. Many such studies have employed various methods to mimic the dosimetric impact of setup errors. These methods include dose simulation on planning computed tomography (pCT), cone-beam CT (CBCT), and dose accumulation using deformable image registration of pCT and CBCT [22–32]. Most previous studies simulated and evaluated the dosimetric impact of interfractional setup errors on pCT with weekly or lower imaging frequencies of setup verification [22–29]. The dosimetric impact of 6-dimensional (6D) interfractional setup errors in head and neck cancer has been studied in previous studies. In these studies, the dosimetric impact on pCT was based on the assumption that there was no geometric variation over the entire treatment course [22, 24, 27, 28, 30]. However, interfractional geometric variation could occur throughout the treatment [33, 34]. The CBCT acquired for pretreatment setup verification provides the actual patient volumes at the treatment fraction. CBCT-based dose reconstruction could provide the actual dose delivered to the patient in the treatment fraction. Previous studies have reported on the feasibility and accuracy of CBCT for treatment dose simulation [35–42].

Evaluation of the dosimetric impact of 6D interfractional setup errors on verification CBCT is highly relevant as CBCT characterizes the actual patient's volumes at the treatment. Similarly,

Otsuka et al. evaluated the dosimetric impact of parotid and mandible rotation in oropharyngeal cancer using CBCT dose reconstruction. However, the dosimetric impact was evaluated with a limited CBCT dataset [31]. Most radiotherapy clinics perform verification imaging for the first three days and then weekly or less frequently (moderate setup error correction) for IMRT and VMAT [20, 25, 27–29, 31]. However, in tongue (head and neck) cancer, it is important to use daily CBCT to see how the daily interfractional setup error affects the dose.

There is no comprehensive study evaluating how 6D interfractional setup errors affect the dose in tongue cancer patients utilizing daily kilovoltage CBCT dose reconstruction. This study aimed to evaluate the dosimetric impact of daily rotational, translational, and translational plus rotational (6D) errors on target volumes and OARs by using daily kilovoltage CBCT (kV-CBCT).

Materials and methods

Patient characteristics

This retrospective dosimetric study included 20 patients diagnosed with squamous cell carcinoma of the tongue (Stage = T1N0M0–T2N1M0). The study population consisted of fifteen males and five females with a median age of 61 years (range 35–72). Patients underwent definitive radiation therapy by IMRT (10) and VMAT (10) with daily kV-CBCT image guidance. The PerfectPitch 6D robotic couch on the Varian TrueBeam STx linear accelerator was used to correct the setup errors.

Patient simulation and treatment planning

Patients were simulated supine and immobilized with five-clamp head and neck thermoplastic masks with individualized low-density headrests (Orfit Industries, Wijnegem, Belgium). Patients were advised to keep their tongues straight up and not swallow to minimize tongue dislocation during treatment. The pCT scans were acquired on a Biograph mCT flow helical positron emission tomography/computed tomography (PET-CT) scanner (Siemens Medical Systems, Erlangen, Germany) with a 3 mm slice thickness and transferred to the Eclipse treatment planning system (TPS) (v. 13.7, Varian Medical System, Palo Alto, United States). The planning target volume (PTV)

PTV-60, the intermediate-risk PTV, and PTV-54, the low-risk PTV, were prescribed with 60 Gy and 54 Gy in 30 fractions, respectively. PTV was prescribed to receive a minimum of 95% dose and a maximum of 2% volume more than 107% dose. The maximum dose constraint prescribed for the brainstem, spinalcord, and mandible was 54 Gy, 45 Gy, and 65 Gy. The mean dose constraints prescribed for the parotids and the larynx were 26 Gy and 45 Gy, respectively. Treatment plans with 6MV photon energy were optimized for IMRT (7–9 fields) and VMAT (2–3 co-planer full arcs) treatment techniques with a 5 mm target margin in TPS. Dose calculation was done with an analytical anisotropic algorithm (AAA) using a 2.5 mm dose grid.

Image acquisition and evaluation of interfractional 6D setup error

kV-CBCT imaging was used for pretreatment patient positional verification for each fraction. The kV-CBCTs were acquired with an onboard imaging (OBI) system (Varian Medical Systems, Palo Alto, United States) on the TrueBeam STx Linac. The CBCT images were acquired in full-fan mode with 100 kV and 270 mAs in full trajectory. All the images were acquired with a 3 mm slice thickness and had a sufficient scan length to encompass the full target volume. CBCT and pCT images were registered based on bony structure and soft-tissue contrast with the registration software. The 6D setup errors were assessed in the lateral (X), longitudinal (Y), and vertical (Z) principal translation axes, as well as the pitch (R_x), roll (R_y), and yaw (R_z) rotation axes along the principal translation axes. The 6D setup errors of all patients with 600 kV-CBCTs were assessed and used for the evaluation of the dosimetric influence of uncorrected 6D setup errors.

Dose metrics evaluated for target volumes and OARs

The dosimetric influence of rotation error (R_{Error}), translation error (T_{Error}) and 6D translation plus rotation error ($T+R_{Error}$) was evaluated for clinical target volumes (CTV) CTV-60, CTV-54, PTV-60, and PTV-54 with a dose metric of $D_{98\%}$ (dose to 98% of volume), $D_{95\%}$, $D_{2\%}$, and $D_{0.035cc}$ (dose to 0.035 cc volume, a near-maximum dose) on the dose-volume histogram (DVH).

The OARs: spinalcord, brainstem, and mandible were evaluated for dose metrics of D_{1cc} and $D_{0.035cc}$. Left parotid, right parotid, and larynx were evaluated for the dose metrics D_{mean} (mean dose in volume) and $D_{50\%}$.

Treatment plan simulation with 6D setup errors using kV-CBCT

The pCT structure set was deformed to CBCT using Varian's demons deformable image registration (DIR) implemented in SmartAdapt (SA) (v.13.7, Varian Medical System, Palo Alto, CA, United States) in Eclipse TPS. A radiation oncologist evaluated the deformed structures on CBCT for accuracy and integrity. Pretreatment CBCT images inherently contain translation and rotation setup errors if they exist in the treatment setup. Similarly, CBCT images contain the interfraction geometric (external as well as internal organ) variation if it exists. However, we aimed to investigate the influence of only uncorrected setup errors on the delivered doses of the treatment plans. To eliminate the effect of geometric variation (external body) on evaluating the dosimetric influence of setup errors, a reference CBCT structure set (CBCT_REF) without 6D setup errors was generated on pre-treatment CBCT. However, the internal geometric variations were accounted for in the CBCT structure set. The CBCT structures were mapped (copied) on pCT with rigid registration and re-mapped back onto CBCT from pCT without rotational correction in the rigid registration. The workflow is illustrated in Figure 1. The original treatment plan on pCT (Fig. 2AB) was recalculated using CBCT_REF, utilizing beam parameters, monitor units, and fluence maps from the original plan. A previously evaluated and validated HU to ED conversion curve for head and neck CBCT in our institute was used for dose calculation [42]. This plan without 6D setup errors was referred to as the reference plan (Ref). The treatment plan R with rotation error (R_{Error}) alone was simulated on pretreatment CBCT without translation error (T_{Error}), illustrated in Figures 2CD (Example). The treatment plan T+R with 6D translation plus rotation error ($T+R_{Error}$) was simulated on a pretreatment CBCT with $T+R_{Error}$. The treatment plan T with T_{Error} alone was simulated on the CBCT_REF structure set.

The dosimetric influence of R_{Error} , T_{Error} , and $T+R_{Error}$ was evaluated by comparing the refer-

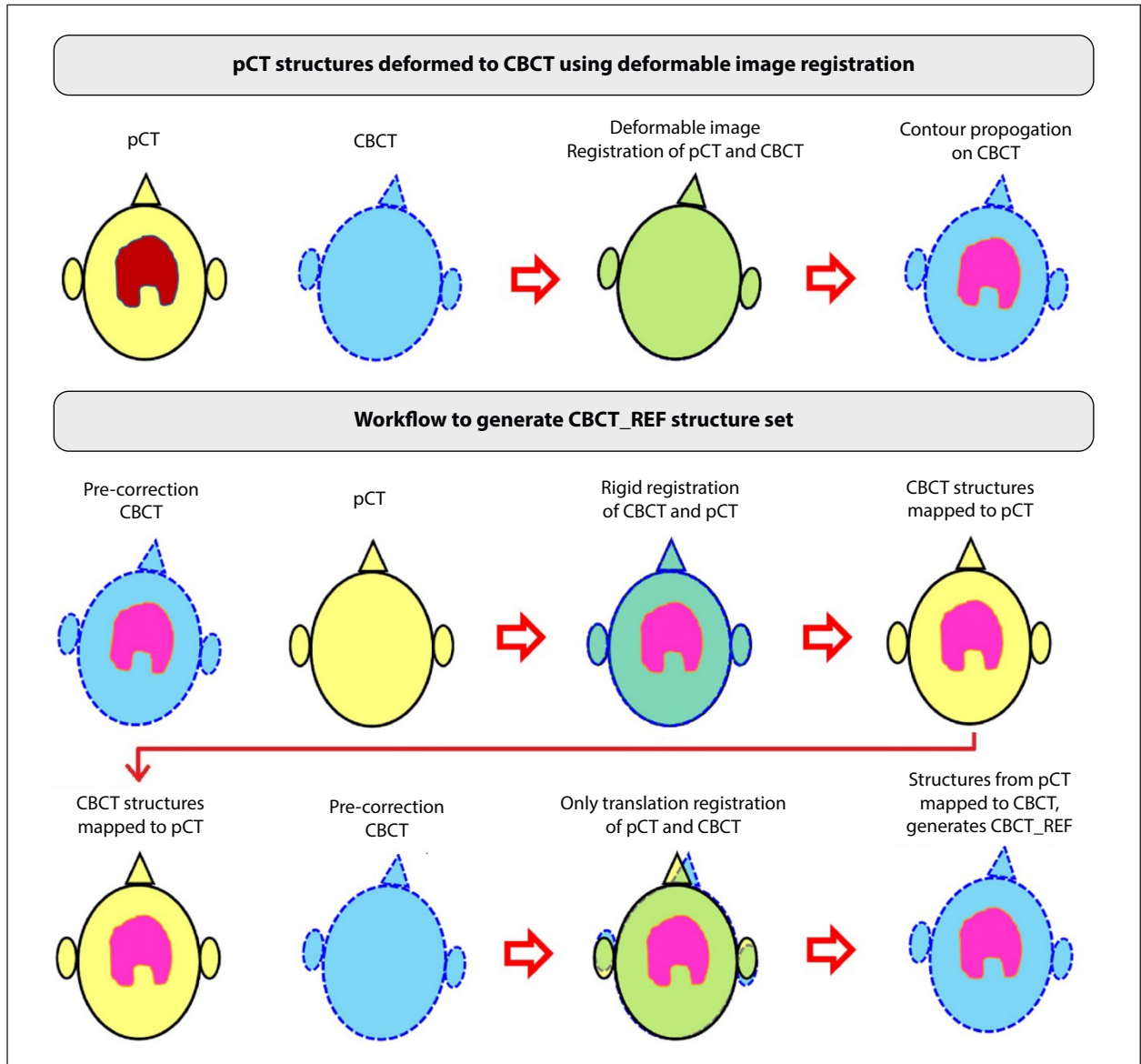


Figure 1. Workflow to deform planning computed tomography (pCT) structure-set to cone-beam computed tomography (CBCT) and to generate CBCT_REF structure set

ence plan (Ref) with R_{Error} (R), T_{Error} (T), and $T+R_{Error}$ (T+R) plans on CBCT. For each fraction, the percentage dose variation in the R_{Error} plan (δD_R (%)), T_{Error} plan (δD_T (%)), and $T+R_{Error}$ plan (δD_{T+R} (%)) in the evaluated target volumes and OARs for the corresponding dose metrics were calculated.

The mean percentage dose variation ΔD_R (%), ΔD_T (%), and ΔD_{T+R} (%) due to R_{Error} , T_{Error} , and $T+R_{Error}$, respectively, for all evaluated structures and the corresponding dose metric of all patients were calculated. The absolute dose variation in Gray (Gy) owing to R_{Error} , T_{Error} , and $T+R_{Error}$ in original treatment plan on pCT

was calculated by applying the corrections with % dose variation δD_R (%), δD_T (%), and δD_{T+R} (%) to the DVH of the corresponding structures and dose metrics in each fraction of the treatment plan. The mean absolute dose variation in ΔD_R (Gy), ΔD_T (Gy), and ΔD_{T+R} (Gy) due to R_{Error} , T_{Error} , and $T+R_{Error}$, respectively, for the corresponding evaluated structures and dose metrics was calculated for all patients. The dosimetric influence of 6D setup error was evaluated for no setup error correction and moderate setup error correction (first three days and weekly once thereafter) approach.

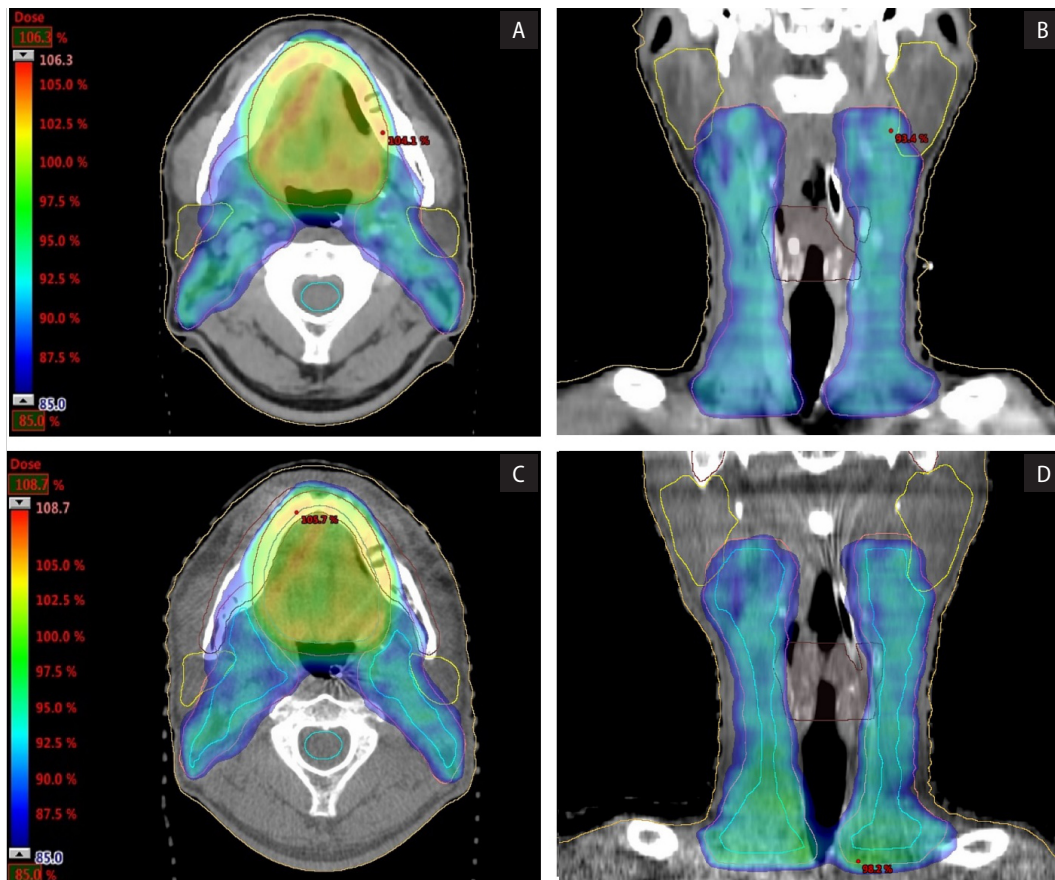


Figure 2. Original treatment plan dose distribution for planning target volume (PTV): PTV-60 and PTV-54 on (A) axial computed tomography (CT) image and (B) coronal CT image, and recalculated dose distribution with rotational error for PTV-60 and PTV-54 on (C) axial cone-beam computed tomography (CBCT) image and (D) coronal CBCT image, for a single fraction.

Statistical analysis

The mean absolute dose D_p (Gy) of the evaluated structures for each dose metric (e.g., CTV-60 for dose metrics $D_{98\%}$, $D_{95\%}$, $D_{2\%}$, and $D_{0.03cc}$) in the original treatment plan of 20 patients was compared to the mean absolute doses D_R (Gy), D_T (Gy), and D_{T+R} (Gy) in the R_{Error} plan, T_{Error} plan, and $T+R_{Error}$ plan, respectively. Statistical analysis was done in Microsoft Excel. The two-tailed paired t-test was used to test the hypothesis that there was no difference between the D_p (Gy) and D_R (Gy), D_p (Gy) and D_T (Gy), and D_p (Gy) and D_{T+R} (Gy) for the evaluated structures and dose metrics in 20 patients with $\alpha = 0.05$.

Results

Assessment of the 6D setup error

A total of 600 pretreatment kV-CBCTs were evaluated for 6D setup error analysis. The Van

Herk PTV margin (Margin = $2.5 \Sigma + 0.7 \sigma$) [43] for population systematic (Σ) and random (σ) error was 4.7 mm, 3.9 mm, and 4.5 mm along the X, Y, and Z axes, respectively. The single fraction maximum error was 7 mm, 7 mm, 8 mm, 3.0° , 2.9° , and 2.9° along the X, Y, Z, R_x , R_y , and R_z axes, respectively.

Dosimetric influence of the 6D setup error

Figure 3 depicts a single fraction DVH comparison for patient 1 between a reference plan (Ref) with no setup error and plan ‘R’ with R_{Error} , plan ‘T’ with T_{Error} , and plan ‘T+R’ with 6D $T+R_{Error}$. The dose variation in the target volume and OARs due to R_{Error} , T_{Error} , and $T+R_{Error}$ is realized in Figures 3A–C, respectively. The mean % dose variation ΔD_R (%), ΔD_T (%), and ΔD_{T+R} (%) in targets and OARs for the corresponding evaluated dose metrics with no setup error correction in all fractions and with

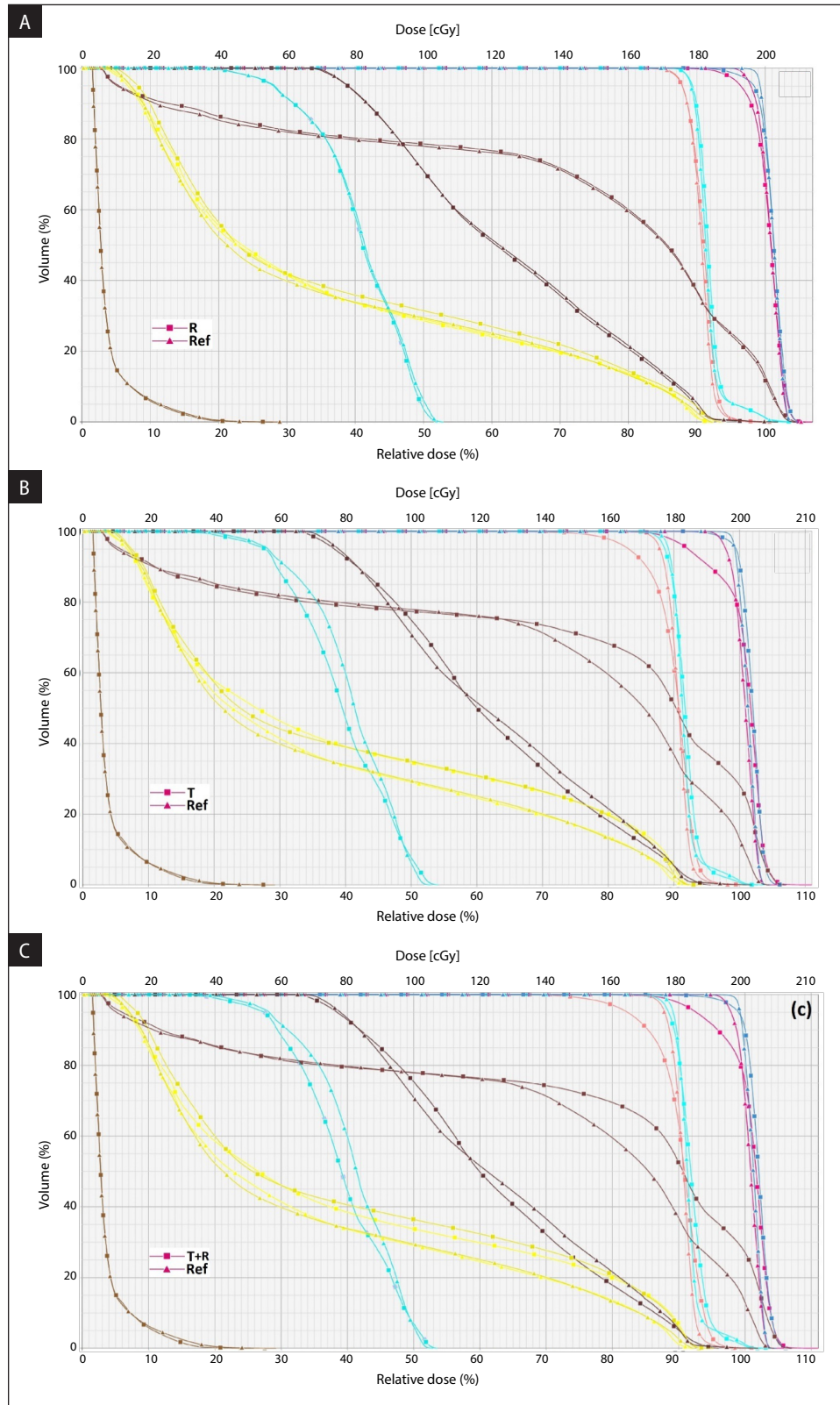


Figure 3. Dose volume histogram comparison for a single fraction of patient-1 for (A) reference plan (Ref) and rotational error plan (R), (B) reference plan (Ref) and translational error plan (T), and (C) reference plan (Ref) and translational plus rotational error plan (T+R). DVH color: clinical target volume (CTV): CTV-60 (dark blue), CTV-54 (cyan), planning target volume (PTV): PTV-60 (pink), PTV-54 (orange), parotid-right, and parotid-left (yellow), brainstem (brown), spinalcord (cyan), mandible and larynx (dark brown). Dose volume histogram (DVH) marker: reference plan (triangle) and setup error plan (square)

Table 1. The overall mean percentage dose variation in targets and organs at risk (OARs) for the corresponding evaluated dose metrics in 20 patients with no setup error correction and moderate setup error correction approach

ROI	Dose-index	With no setup error correction			With moderate setup error correction		
		ΔD_R (%) Mean \pm SD	ΔD_T (%) Mean \pm SD	ΔD_{T+R} (%) Mean \pm SD	ΔD_R (%) Mean \pm SD	ΔD_T (%) Mean \pm SD	ΔD_{T+R} (%) Mean \pm SD
CTV-60	D _{98%}	-0.3 \pm 0.2	-0.4 \pm 0.3	-0.6 \pm 0.3	-0.2 \pm 0.1	-0.3 \pm 0.2	-0.5 \pm 0.3
	D _{95%}	-0.1 \pm 0.1	-0.3 \pm 0.2	-0.4 \pm 0.3	-0.1 \pm 0.1	-0.2 \pm 0.2	-0.3 \pm 0.2
	D _{2%}	0.2 \pm 0.1	0.3 \pm 0.3	0.5 \pm 0.3	0.1 \pm 0.1	0.2 \pm 0.3	0.3 \pm 0.3
	D _{0.035cc}	0.6 \pm 0.9	0.7 \pm 0.6	1.3 \pm 1.2	0.4 \pm 0.6	0.6 \pm 0.4	1.1 \pm 1.0
CTV-54	D _{98%}	-0.2 \pm 0.4	-0.4 \pm 0.6	-0.6 \pm 0.5	-0.1 \pm 0.3	-0.3 \pm 0.5	-0.4 \pm 0.5
	D _{95%}	-0.2 \pm 0.5	-0.2 \pm 0.5	-0.4 \pm 0.5	-0.1 \pm 0.3	-0.2 \pm 0.4	-0.3 \pm 0.4
	D _{2%}	0.4 \pm 0.5	0.7 \pm 0.6	1.1 \pm 0.6	0.3 \pm 0.4	0.5 \pm 0.5	0.8 \pm 0.4
	D _{0.035cc}	0.7 \pm 1.1	1.2 \pm 0.8	1.9 \pm 0.7	0.5 \pm 0.8	0.8 \pm 0.7	1.4 \pm 0.5
PTV-60	D _{98%}	-0.6 \pm 0.5	-4.0 \pm 2.6	-4.5 \pm 2.8	-0.5 \pm 0.4	-3.0 \pm 2.0	-3.4 \pm 2.2
	D _{95%}	-0.3 \pm 0.3	-2.5 \pm 1.8	-2.7 \pm 2.0	-0.2 \pm 0.2	-1.9 \pm 1.4	-2.1 \pm 1.5
	D _{2%}	0.2 \pm 0.1	0.3 \pm 0.3	0.5 \pm 0.3	0.1 \pm 0.1	0.2 \pm 0.3	0.3 \pm 0.2
	D _{0.035cc}	1.0 \pm 0.9	1.4 \pm 1.3	2.3 \pm 1.5	0.7 \pm 0.6	1.1 \pm 0.9	1.7 \pm 1.2
PTV-54	D _{98%}	-0.6 \pm 0.5	-4.7 \pm 3.1	-5.4 \pm 3.9	-0.4 \pm 0.4	-3.5 \pm 2.5	-4.0 \pm 2.5
	D _{95%}	-0.4 \pm 0.4	-2.4 \pm 2.0	-2.7 \pm 2.0	-0.2 \pm 0.3	-1.8 \pm 1.6	-2.0 \pm 1.7
	D _{2%}	0.4 \pm 0.5	0.8 \pm 0.6	1.2 \pm 0.4	0.3 \pm 0.4	0.5 \pm 0.5	0.9 \pm 0.3
	D _{0.035cc}	1.0 \pm 1.2	1.7 \pm 1.9	2.5 \pm 1.4	0.7 \pm 0.9	1.2 \pm 1.5	1.8 \pm 1.1
Spinalcord	D _{1cc}	0.5 \pm 1.4	0.4 \pm 2.2	0.9 \pm 2.2	0.5 \pm 1.1	0.2 \pm 2.1	0.7 \pm 1.9
	D _{0.035cc}	0.3 \pm 0.4	1.2 \pm 2.6	1.6 \pm 2.8	0.2 \pm 0.3	1.1 \pm 2.3	1.3 \pm 2.4
Brainstem	D _{1cc}	-0.3 \pm 0.7	-1.5 \pm 4.1	-1.9 \pm 4.2	-0.2 \pm 0.6	-1.0 \pm 3.1	-1.2 \pm 3.2
	D _{0.035cc}	-0.5 \pm 0.7	-2.4 \pm 3.3	-3.0 \pm 3.1	-0.4 \pm 0.6	-0.2 \pm 2.5	-2.4 \pm 2.3
Left Parotid	D _{mean}	0.4 \pm 2.2	5.5 \pm 6.1	5.7 \pm 6.2	0.4 \pm 1.1	4.4 \pm 4.6	4.7 \pm 5.0
	D _{50%}	-0.8 \pm 4.7	10.6 \pm 15.2	10.1 \pm 15.9	-0.2 \pm 3.6	7.5 \pm 10.9	7.7 \pm 12.0
Right Parotid	D _{mean}	1.7 \pm 2.5	0.3 \pm 8.3	1.7 \pm 9.2	1.1 \pm 2.0	-0.1 \pm 6.7	1.0 \pm 7.4
	D _{50%}	2.3 \pm 5.1	-0.7 \pm 10.8	2.6 \pm 13.3	2.8 \pm 5.0	-0.2 \pm 7.7	2.4 \pm 10.8
Larynx	D _{mean}	0.2 \pm 0.5	-0.4 \pm 2.1	-0.3 \pm 2.0	0.1 \pm 0.4	-0.5 \pm 1.6	-0.4 \pm 1.5
	D _{50%}	-0.0 \pm 0.4	-0.5 \pm 2.0	-0.4 \pm 2.0	0.1 \pm 0.3	-0.4 \pm 1.6	-0.3 \pm 1.6
Mandible	D _{1cc}	-0.2 \pm 1.2	1.0 \pm 1.4	0.7 \pm 0.6	-0.4 \pm 1.2	0.7 \pm 1.4	0.3 \pm 0.8
	D _{0.035cc}	0.6 \pm 0.5	1.1 \pm 1.0	1.4 \pm 0.9	0.2 \pm 0.3	0.6 \pm 0.8	0.8 \pm 0.9

ROI — region of interest; CTV — clinical target volume; PTV — planning target volume; SD — standard deviation; ΔD_R — dose variation in rotational error plan, ΔD_T — dose variation in translational error plan; ΔD_{T+R} — dose variation in translational plus rotational error plan

a moderate setup error correction approach are summarized in Table 1.

The box and whisker plot in Figure 4 for CTV-60, CTV-54, PTV-60 and PTV-54, and in Figure 5 for Spinal Cord and Brainstem, Left Parotid and Right Parotid, and for Larynx and Mandible depict the percentage dose variation ΔD (%) in the R_{Error} plan (R), T_{Error} plan (T), and 6D T+R_{Error} plan (T+R) on CBCT with respect to the reference plan (Ref) on CBCT_REF for the corresponding evaluated dose metrics with no setup error correction (NC) and moderate setup error correction (MC) in few fractions.

For the no setup error correction and moderate setup error correction approaches, respectively, Table 2 and Table 3 summarized the absolute mean dose D_p (Gy) in the original treatment plan and the D_R (Gy), D_T (Gy), and D_{T+R} (Gy) in the R_{Error}, T_{Error}, and T+R_{Error} plans, respectively, for all CTVs, PTVs, and OARs with the corresponding evaluated dose metrics across all 20 patients. Similarly, Tables 4 and Table 5 summarized the mean percentage dose variation ΔD_R (%), ΔD_T (%), and ΔD_{T+R} (%) for IMRT and VMAT plans in CTVs, PTVs, and OARs for the corresponding

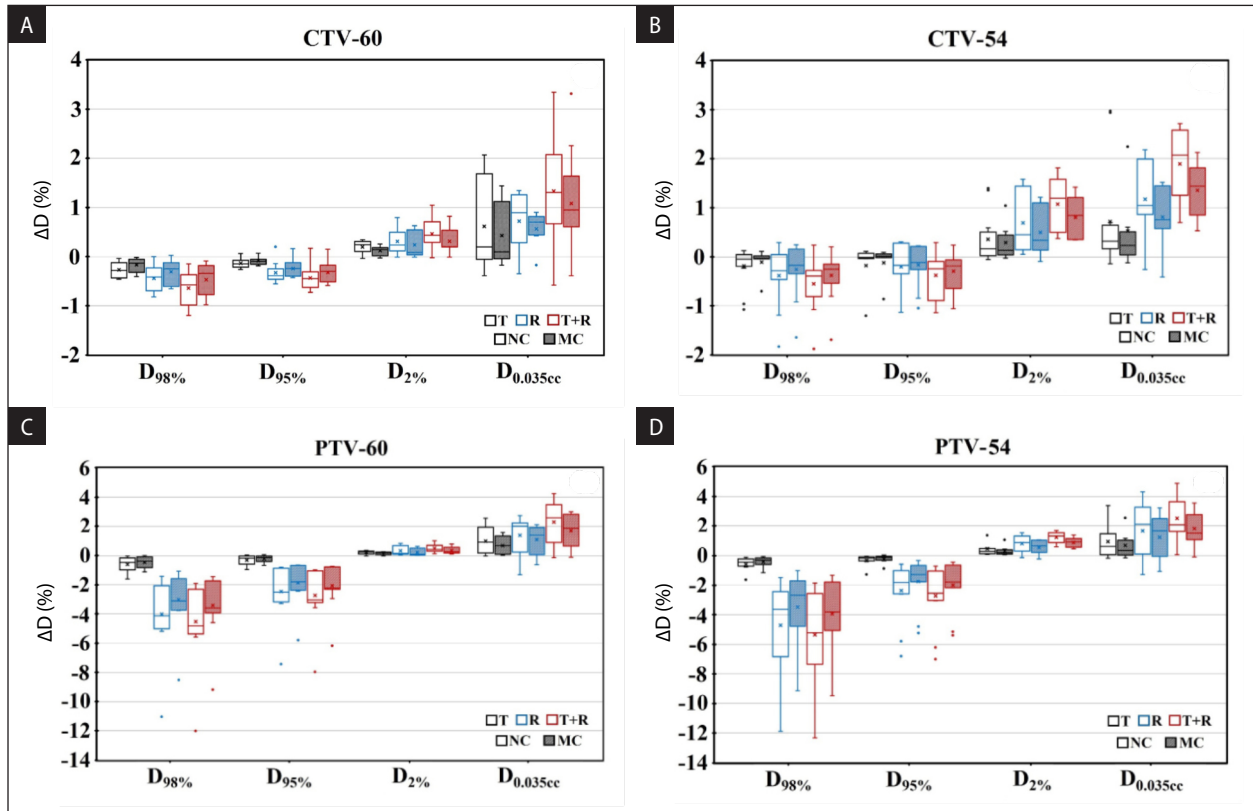


Figure 4. Box and whisker plot for percentage dose variation ΔD (%) in rotational error (R), translational error (T), and translational plus rotational error (T+R) plans with no correction (NC) and moderate correction (MC) of setup errors for $D_{98\%}$, $D_{95\%}$, $D_{2\%}$ and $D_{0.035cc}$ in clinical target volume (CTV): (A) CTV-60, (B) CTV-54, and planning target volume (PTV) (C) PTV-60, and (D) PTV-54. The cross represents the mean, the line inside the box represents the median, the bottom of the box represents the 25% quartile, the top of the box represents the 75% quartile, the bottom whisker represents the minimum value, the top whisker represents the maximum value, and the dots represent the outlier

evaluated dose metrics with no setup error correction and moderate setup error correction approaches, respectively.

Discussion

Interfractional setup errors in ca-tongue are mainly attributed to changes in the patient's position, shape, or size due to weight loss and displacement of the target relative to the skin marks. Geometrical deviations are classified into systematic errors (treatment preparations) and random errors (treatment execution). Systematic error leads to a displacement of the dose distribution, and random error leads to the blurring of the dose distribution with respect to the CTV [43]. Ideally, treatment setup errors cannot be separated into the R_{Error} and T_{Error} . However, R_{Error} and T_{Error} alone were analyzed to evaluate how uncorrected R_{Error} affects the doses to targets and OARs where 6-DoF couch

is not onboard and how uncorrected T_{Error} affects the doses to targets and OARs independently to compare with the previous dosimetric studies that evaluated the dosimetric impact of translational errors on pCT, which did not account for the internal organ geometric variation during the treatment.

The overall population mean error (M_{pop}), systematic error (Σ), and random error (σ) were within 1.2–1.6 mm and 0.1–0.7 degrees. This indicates that the overall average tongue dislocation was smaller. The lateral, longitudinal, and vertical translational axes had CTV to PTV margins of 4.7 mm, 3.9 mm, and 4.5 mm, respectively, which were consistent with earlier studies for the PTV margin in head and neck cancer [13, 18–20]. However, Mesias et al. found a larger PTV margin of 4.9 mm, 6.4 mm, and 5.8 mm in the lateral, longitudinal, and vertical axes, respectively [21].

Figure 2 illustrates the dosimetric impact of uncorrected R_{Error} on the CBCT of patient

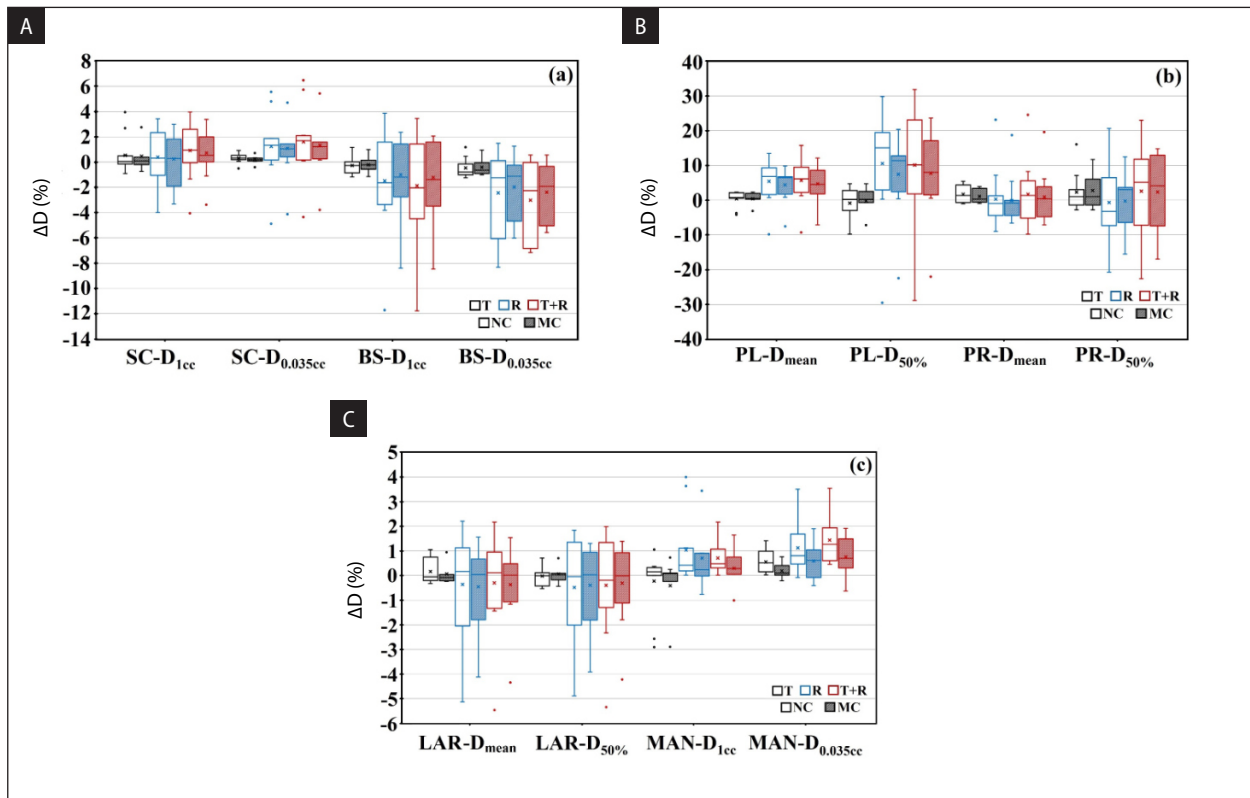


Figure 5. Box and whisker plot for percentage dose variation ΔD (%) in rotational error (R), translational error (T), and translational plus rotational error (T+R) plans with no correction (NC) and moderate correction (MC) of setup errors (A) for D_{1cc} and $D_{0.035cc}$ in the spinalcord (SC) and brainstem (BS), (B) for D_{mean} and $D_{50\%}$ in the parotid-left (PL) and parotid-right (PR), and (C) for D_{mean} and $D_{50\%}$ in the larynx (LAR), and for D_{1cc} and $D_{0.035cc}$ in the mandible (MAN). The cross represents the mean, the line inside the box represents the median, the bottom of the box represents the 25% quartile, the top of the box represents the 75% quartile, the bottom whisker represents the minimum value, the top whisker represents the maximum value, and the dots represent the outlier

1 for a single fraction. Figures 2A and 2B illustrate the original plan dose distribution on pCT. The dose deviation at the periphery of target and OAR volumes due to R_{Error} is clearly visible in Figures 2CD. Figures 3A–C illustrate the DVH comparison for a single fraction of patient 1 for R_{Error} , T_{Error} , and $T+R_{Error}$ respectively, with the reference plan (Ref). The dose deviation in CTVs, PTVs, and OARs is higher in T_{Error} and $T+R_{Error}$ compared to R_{Error} . This is attributed to the larger displacement of treatment volume in T_{Error} and $T+R_{Error}$ with translation error coupled with rotational error. R_{Error} alone generally causes dose variation at the edges or periphery of the target and OAR volumes (Fig. 2CD).

The box and whisker plot in Figures 4 and 5 depict the overall dosimetric impact for the evaluated dose metric in all 20 patients for CTVs, PTVs, and OARs. The outliers depict the maximum deviation in the evaluated dose metrics for CTVs,

PTVs, and OARs. This is attributed to the large setup variations in some patients.

The dosimetric impact of uncorrected R_{Error} , T_{Error} , and $T+R_{Error}$ for all treatment fractions and for moderate correction of R_{Error} , T_{Error} , and $T+R_{Error}$ in the first three fractions and weekly thereafter (Tab. 1) showed a similar nature in targets and OARs. However, the magnitude of percentage dose deviation ΔD_R (%), ΔD_T (%), and ΔD_{T+R} (%) for R_{Error} , T_{Error} , and $T+R_{Error}$ respectively, were slightly lower with moderate setup error correction compared to no setup error correction for all fractions.

The absolute magnitude of mean ΔD (%) in target volumes for $D_{98\%}$, $D_{95\%}$, $D_{2\%}$, and $D_{0.035cc}$ increased with R_{Error} , T_{Error} , and $T+R_{Error}$ (Fig. 4). This can be attributed to the increasing deviation in the congruence between target volume and planned treatment volume with R_{Error} , T_{Error} , and $T+R_{Error}$ respectively. The mean absolute dose (Gy) for $D_{98\%}$ and $D_{95\%}$ was reduced but increased for $D_{2\%}$ and $D_{0.035cc}$ in target

Table 2. Mean dose of the target and organ at risk (OAR) volumes for the corresponding evaluated dose metrics in the original treatment plan and setup error plans for 20 patients with no setup error correction approach

ROI	Dose-index	D_p [Gy]	D_R [Gy]	p^*	D_T [Gy]	p^*	D_{T+R} [Gy]	p^*
		Mean \pm SD	Mean \pm SD		Mean \pm SD		Mean \pm SD	
CTV-60	$D_{98\%}$	59.15 \pm 0.47	58.99 \pm 0.44	< 0.05	58.89 \pm 0.51	< 0.05	58.77 \pm 0.50	< 0.05
	$D_{95\%}$	59.48 \pm 0.52	59.40 \pm 0.52	< 0.05	59.28 \pm 0.51	< 0.05	59.22 \pm 0.51	< 0.05
	$D_{2\%}$	62.50 \pm 0.57	62.63 \pm 0.54	< 0.05	62.70 \pm 0.67	< 0.05	62.79 \pm 0.65	< 0.05
	$D_{0.035cc}$	63.84 \pm 0.52	64.23 \pm 0.57	< 0.05	64.30 \pm 0.56	< 0.05	64.69 \pm 0.72	< 0.05
CTV-54	$D_{98\%}$	53.56 \pm 0.77	53.46 \pm 0.85	0.136	53.35 \pm 0.75	< 0.05	53.26 \pm 0.78	< 0.05
	$D_{95\%}$	53.79 \pm 0.75	53.69 \pm 0.84	0.214	53.68 \pm 0.74	0.173	53.59 \pm 0.79	< 0.05
	$D_{2\%}$	56.08 \pm 0.89	56.27 \pm 0.82	< 0.05	56.47 \pm 1.13	< 0.05	56.68 \pm 1.03	< 0.05
	$D_{0.035cc}$	56.69 \pm 0.92	57.09 \pm 0.92	< 0.05	57.36 \pm 1.17	< 0.05	57.76 \pm 0.96	< 0.05
PTV-60	$D_{98\%}$	57.97 \pm 0.41	57.62 \pm 0.54	< 0.05	55.64 \pm 1.43	< 0.05	55.34 \pm 1.58	< 0.05
	$D_{95\%}$	58.77 \pm 0.41	58.58 \pm 0.49	< 0.05	57.32 \pm 1.02	< 0.05	57.16 \pm 1.11	< 0.05
	$D_{2\%}$	62.55 \pm 0.58	62.68 \pm 0.55	< 0.05	62.75 \pm 0.64	< 0.05	62.86 \pm 0.64	< 0.05
	$D_{0.035cc}$	64.38 \pm 0.62	65.01 \pm 0.88	< 0.05	65.26 \pm 0.76	< 0.05	65.85 \pm 1.06	< 0.05
PTV-54	$D_{98\%}$	52.96 \pm 0.57	52.65 \pm 0.63	< 0.05	50.46 \pm 1.57	< 0.05	50.12 \pm 1.61	< 0.05
	$D_{95\%}$	53.45 \pm 0.63	53.26 \pm 0.70	< 0.05	52.17 \pm 1.08	< 0.05	51.99 \pm 1.14	< 0.05
	$D_{2\%}$	56.30 \pm 0.92	56.55 \pm 0.82	< 0.05	56.76 \pm 1.15	< 0.05	57.00 \pm 1.02	< 0.05
	$D_{0.035cc}$	58.32 \pm 1.23	58.87 \pm 1.12	< 0.05	59.31 \pm 2.02	< 0.05	59.79 \pm 1.61	< 0.05
Spinalcord	D_{1cc}	33.65 \pm 2.59	33.82 \pm 2.48	0.200	33.82 \pm 3.14	0.440	33.98 \pm 3.05	0.151
	$D_{0.035cc}$	36.45 \pm 2.32	36.57 \pm 2.41	< 0.05	36.93 \pm 2.99	0.108	37.07 \pm 3.09	0.061
Brainstem	D_{1cc}	26.58 \pm 9.48	26.47 \pm 9.70	0.061	26.19 \pm 9.70	0.164	26.05 \pm 9.57	0.091
	$D_{0.035cc}$	31.91 \pm 9.88	31.73 \pm 9.76	< 0.05	31.14 \pm 9.61	< 0.05	30.93 \pm 9.48	< 0.05
Left parotid	D_{mean}	30.90 \pm 9.41	30.92 \pm 9.52	0.895	32.32 \pm 9.03	< 0.05	32.47 \pm 9.32	< 0.05
	$D_{50\%}$	28.61 \pm 16.44	28.47 \pm 16.57	0.581	30.93 \pm 16.9	0.132	30.96 \pm 17.3	0.143
Right parotid	D_{mean}	27.43 \pm 3.22	27.88 \pm 3.16	< 0.05	27.46 \pm 3.40	0.969	27.81 \pm 3.45	0.605
	$D_{50\%}$	22.73 \pm 6.20	23.19 \pm 6.09	0.168	22.38 \pm 5.75	0.598	23.08 \pm 5.85	0.687
Larynx	D_{mean}	44.96 \pm 3.81	45.04 \pm 3.94	0.277	44.79 \pm 3.83	0.535	44.83 \pm 3.93	0.595
	$D_{50\%}$	44.87 \pm 5.24	44.87 \pm 5.36	0.988	44.67 \pm 5.33	0.402	44.71 \pm 5.42	0.506
Mandible	D_{1cc}	61.92 \pm 0.52	61.78 \pm 0.66	0.518	62.56 \pm 1.09	< 0.05	62.36 \pm 0.46	< 0.05
	$D_{0.035cc}$	62.87 \pm 0.64	63.21 \pm 0.53	< 0.05	63.57 \pm 0.80	< 0.05	63.77 \pm 0.70	< 0.05

ROI — region of interest; CTV — clinical target volume; PTV — planning target volume; SD — standard deviation; D_p — dose in original treatment plan; D_R — dose in rotational error plan; D_T — dose in translational error plan; D_{T+R} — dose in translational plus rotational error plan; *two tailed paired t test with significance value $p < 0.05$

volumes with R_{Error} , T_{Error} and $T+R_{Error}$ and was statistically significant ($p < 0.05$) (Tab. 2, 3). This can be attributed to the increasing deviation of target volume from planned treatment volume. This results in underdosing of target volume and increasing the high dose volume within the target volume due to highly conformal dose of IMRT and VMAT plans. Kaur et al. [29] also reported similar results for uncorrected T_{Error} with a significant p-value in head and neck cancer. Our results for R_{Error} concur with Fu et al. [28] who reported a similar result for $D_{98\%}$ in CTV and $D_{95\%}$ in PTV for R_{Error} . Jiang

et al. [30] reported similar results for $D_{98\%}$ and $D_{95\%}$ in PTV for $T+R_{Error}$.

The mean absolute dose (Gy) variations ΔD_R , ΔD_T and ΔD_{T+R} in Spinalcord for $D_{0.035cc}$ were 0.12 ± 0.13 Gy, 0.48 ± 0.96 Gy, and 0.62 ± 1.03 Gy, respectively, with no setup error correction. This can be attributed to the increasing deviation in congruence between the target volume and the planned treatment volume with R_{Error} , T_{Error} and $T+R_{Error}$, respectively. Kaur et al. [29] also reported similar results for an uncorrected T_{Error} . However, for R_{Error} Fu et al. [28]

Table 3. Mean dose of the target and organ at risk (OAR) volumes for the corresponding evaluated dose metrics in the original treatment plan and setup error plans for 20 patients with moderate setup error correction approach

ROI	Dose-index	D _p [Gy] Mean ± SD	D _r [Gy] Mean ± SD	p*	D _r [Gy] Mean ± SD	p*	D _{T+R} [Gy] Mean ± SD	p*
CTV-60	D _{98%}	59.13 ± 0.47	59.03 ± 0.44	< 0.05	58.94 ± 0.50	< 0.05	58.85 ± 0.48	< 0.05
	D _{95%}	59.47 ± 0.52	59.42 ± 0.52	< 0.05	59.32 ± 0.51	< 0.05	59.28 ± 0.51	< 0.05
	D _{2%}	62.53 ± 0.56	62.61 ± 0.55	< 0.05	62.68 ± 0.62	< 0.05	62.72 ± 0.62	< 0.05
	D _{0.035cc}	63.84 ± 0.52	64.11 ± 0.47	< 0.05	64.20 ± 0.52	< 0.05	64.53 ± 0.60	< 0.05
CTV-54	D _{98%}	53.56 ± 0.77	53.48 ± 0.82	0.160	53.40 ± 0.77	0.142	53.33 ± 0.80	< 0.05
	D _{95%}	53.79 ± 0.75	53.72 ± 0.81	0.224	53.69 ± 0.73	0.209	53.63 ± 0.77	< 0.05
	D _{2%}	56.08 ± 0.89	56.23 ± 0.83	< 0.05	56.35 ± 1.07	< 0.05	56.52 ± 0.99	< 0.05
	D _{0.035cc}	56.69 ± 0.92	57.00 ± 0.88	< 0.05	57.16 ± 1.12	< 0.05	57.47 ± 0.95	< 0.05
PTV-60	D _{98%}	57.97 ± 0.41	57.71 ± 0.50	< 0.05	56.22 ± 1.11	< 0.05	56.00 ± 1.22	< 0.05
	D _{95%}	58.77 ± 0.41	58.63 ± 0.46	< 0.05	57.67 ± 0.81	< 0.05	57.55 ± 0.88	< 0.05
	D _{2%}	62.55 ± 0.58	62.65 ± 0.56	< 0.05	62.69 ± 0.62	< 0.05	62.78 ± 0.62	< 0.05
	D _{0.035cc}	64.38 ± 0.62	64.81 ± 0.75	< 0.05	65.07 ± 0.64	< 0.05	65.47 ± 0.86	< 0.05
PTV-54	D _{98%}	52.96 ± 0.57	52.74 ± 0.60	< 0.05	51.12 ± 1.23	< 0.05	50.87 ± 1.27	< 0.05
	D _{95%}	53.45 ± 0.63	53.31 ± 0.68	< 0.05	52.50 ± 0.93	< 0.05	52.36 ± 0.98	< 0.05
	D _{2%}	56.30 ± 0.92	56.50 ± 0.84	< 0.05	56.63 ± 1.10	< 0.05	56.81 ± 1.00	< 0.05
	D _{0.035cc}	58.32 ± 1.23	58.72 ± 1.10	< 0.05	59.05 ± 1.82	< 0.05	59.39 ± 1.50	< 0.05
Spinalcord	D _{1cc}	33.65 ± 2.59	33.82 ± 2.46	0.124	33.79 ± 3.08	0.506	33.94 ± 2.96	0.122
	D _{0.035cc}	36.45 ± 2.32	36.52 ± 2.38	< 0.05	36.86 ± 2.87	0.117	36.95 ± 2.94	0.007
Brainstem	D _{1cc}	26.58 ± 9.48	27.05 ± 10.17	0.008	26.93 ± 10.29	0.354	26.83 ± 10.21	0.241
	D _{0.035cc}	31.91 ± 9.88	31.77 ± 9.77	< 0.05	31.31 ± 9.67	< 0.05	31.15 ± 9.54	< 0.05
Left parotid	D _{mean}	30.90 ± 9.41	30.93 ± 9.48	0.317	31.95 ± 9.08	< 0.05	32.10 ± 9.32	< 0.05
	D _{50%}	28.61 ± 16.44	28.45 ± 16.49	1.000	30.00 ± 16.42	0.181	30.16 ± 16.68	0.178
Right parotid	D _{mean}	27.43 ± 3.22	27.81 ± 3.21	0.116	27.42 ± 3.20	0.716	27.71 ± 3.25	0.882
	D _{50%}	22.73 ± 6.20	23.01 ± 6.15	0.117	22.23 ± 5.68	0.546	22.77 ± 5.75	0.752
Larynx	D _{mean}	44.96 ± 3.81	45.05 ± 3.93	0.447	44.80 ± 3.79	0.386	44.85 ± 3.89	0.463
	D _{50%}	44.87 ± 5.24	44.88 ± 5.35	0.270	44.67 ± 5.28	0.541	44.72 ± 5.37	0.713
Mandible	D _{1cc}	61.92 ± 0.52	59.92 ± 4.23	0.257	60.62 ± 4.75	0.124	62.37 ± 4.59	0.231
	D _{0.035cc}	62.87 ± 0.64	61.82 ± 3.30	0.075	62.07 ± 3.50	< 0.05	62.18 ± 3.59	< 0.05

ROI — region of interest; CTV — clinical target volume; PTV — planning target volume; SD — standard deviation; D_p — dose in original treatment plan; D_r — dose in rotational error plan; D_r — dose in translational error plan; D_{T+R} — dose in translational plus rotational error plan; *two tailed paired t test with significance value p < 0.05

reported a higher value of 1.2 ± 1.76 Gy for D_{1cc} than our finding of 0.53 ± 1.38 Gy. Similarly, Jiang et al. [30] found a higher value of 1.85 ± 1.26 Gy for D_{1cc} in cervical spine tumors in head and neck cancer when the spine was within the tumor volume. The maximum mean absolute dose (Gy) variation of D_{0.035cc} in the spinal cord, brainstem, and mandible was 0.62 ± 1.03 Gy, -0.97 ± 1.09 Gy, and 0.90 ± 0.59 Gy in ΔD_{T+R} in 20 patients. The maximum mean absolute dose variation of D_{mean} in the Left Parotid, Right Parotid, and Larynx was 1.6 ± 1.8 Gy, 0.45 ± 0.68 Gy,

and -0.17 ± 0.90 Gy in ΔD_{T+R} , ΔD_R , and ΔD_T , respectively.

The reduction in D_R (Gy), D_T (Gy), and D_{T+R} (Gy) with respect to D_p (Gy) for D_{98%} and D_{95%} in CTV-60, CTV-54, PTV-60, and PTV-54 was statistically significant (p < 0.05) except for D_R (Gy) and D_T (Gy) in CTV-54 for uncorrected (Tab. 2) and moderately corrected setup errors (Tab. 3). The increase in D_R (Gy), D_T (Gy), and D_{T+R} (Gy) with respect to D_p (Gy) for D_{2%} and D_{0.035cc} in CTV-60, CTV-54, PTV-60, and PTV-54, was statistically significant (p < 0.05) (Tab. 2, 3).

Table 4. The overall mean percentage dose variation in targets and organ at risk (OARs) for 10 intensity-modulated radiation therapy (IMRT) and 10 volumetric modulated arc therapy (VMAT) patients for corresponding dose metrics with no setup error correction approach

ROI	Dose-index	IMRT (N=10)			VMAT (N=10)		
		ΔD_R (%) Mean \pm SD	ΔD_T (%) Mean \pm SD	ΔD_{T+R} (%) Mean \pm SD	ΔD_R (%) Mean \pm SD	ΔD_T (%) Mean \pm SD	ΔD_{T+R} (%) Mean \pm SD
CTV-60	D _{98%}	-0.34 \pm 0.16	-0.36 \pm 0.27	-0.64 \pm 0.41	-0.20 \pm 0.12	-0.52 \pm 0.22	-0.64 \pm 0.28
	D _{95%}	-0.18 \pm 0.06	-0.25 \pm 0.25	-0.41 \pm 0.32	-0.10 \pm 0.10	-0.40 \pm 0.12	-0.46 \pm 0.16
	D _{2%}	0.15 \pm 0.15	0.43 \pm 0.33	0.57 \pm 0.39	0.24 \pm 0.09	0.19 \pm 0.09	0.35 \pm 0.14
	D _{0.035cc}	0.53 \pm 0.81	0.55 \pm 0.47	1.07 \pm 0.92	0.70 \pm 1.07	0.88 \pm 0.68	1.59 \pm 1.538
CTV-54	D _{98%}	0.04 \pm 0.08	-0.71 \pm 0.66	-0.69 \pm 0.66	-0.41 \pm 0.48	-0.06 \pm 0.32	-0.41 \pm 0.38
	D _{95%}	0.05 \pm 0.06	-0.51 \pm 0.47	-0.47 \pm 0.47	-0.41 \pm 0.60	0.10 \pm 0.29	-0.29 \pm 0.52
	D _{2%}	0.20 \pm 0.21	0.76 \pm 0.52	1.00 \pm 0.57	0.51 \pm 0.68	0.62 \pm 0.73	1.15 \pm 0.56
	D _{0.035cc}	0.30 \pm 0.27	1.39 \pm 0.53	1.74 \pm 0.77	1.13 \pm 1.42	0.95 \pm 1.05	2.03 \pm 0.61
PTV-60	D _{98%}	-0.72 \pm 0.58	-4.32 \pm 3.59	-4.82 \pm 3.78	-0.50 \pm 0.43	-3.71 \pm 1.59	-4.24 \pm 1.65
	D _{95%}	-0.41 \pm 0.36	-2.74 \pm 2.47	-3.03 \pm 2.64	-0.25 \pm 0.27	-2.21 \pm 1.09	-2.44 \pm 1.09
	D _{2%}	0.16 \pm 0.14	0.50 \pm 0.33	0.62 \pm 0.37	0.25 \pm 0.09	0.13 \pm 0.10	0.36 \pm 0.11
	D _{0.035cc}	0.93 \pm 0.95	0.98 \pm 1.53	1.75 \pm 1.36	1.04 \pm 0.94	1.78 \pm 0.85	2.83 \pm 1.56
PTV-54	D _{98%}	-0.46 \pm 0.19	-6.02 \pm 3.76	-6.58 \pm 3.77	-0.71 \pm 0.71	-3.41 \pm 1.85	-4.14 \pm 2.12
	D _{95%}	-0.20 \pm 0.12	-3.28 \pm 2.45	-3.53 \pm 2.49	-0.50 \pm 0.58	-1.49 \pm 0.73	-1.94 \pm 1.09
	D _{2%}	0.26 \pm 0.14	0.84 \pm 0.44	1.12 \pm 0.43	0.63 \pm 0.61	0.76 \pm 0.76	1.35 \pm 0.27
	D _{0.035cc}	0.60 \pm 0.61	2.18 \pm 1.65	2.56 \pm 1.71	1.30 \pm 1.64	1.16 \pm 2.22	2.45 \pm 1.22
Spinalcord	D _{1cc}	-0.16 \pm 0.41	-0.23 \pm 2.17	-0.27 \pm 2.27	1.23 \pm 1.69	1.03 \pm 2.22	2.10 \pm 1.54
	D _{0.035cc}	0.20 \pm 0.38	-0.32 \pm 2.34	-0.09 \pm 2.22	0.43 \pm 0.29	2.80 \pm 1.90	3.29 \pm 2.21
Brainstem	D _{1cc}	-0.10 \pm 0.73	-2.83 \pm 4.55	-2.96 \pm 4.64	-0.42 \pm 0.66	-0.15 \pm 3.37	-0.81 \pm 3.75
	D _{0.035cc}	-0.25 \pm 0.83	-3.21 \pm 3.22	-3.53 \pm 2.76	-0.71 \pm 0.58	-1.68 \pm 3.51	-2.51 \pm 3.58
L Parotid	D _{mean}	1.13 \pm 0.79	4.44 \pm 8.13	5.48 \pm 8.65	-0.34 \pm 2.88	6.49 \pm 3.54	5.99 \pm 3.28
	D _{50%}	1.95 \pm 2.13	5.50 \pm 18.48	7.25 \pm 19.63	-3.61 \pm 5.13	15.68 \pm 10.07	13.03 \pm 12.33
R Parotid	D _{mean}	-0.05 \pm 1.13	1.88 \pm 11.87	1.78 \pm 12.78	3.44 \pm 2.20	-1.23 \pm 2.17	1.59 \pm 4.71
	D _{50%}	-0.10 \pm 2.47	-0.60 \pm 14.95	0.49 \pm 16.12	4.69 \pm 6.14	-1.97 \pm 5.55	5.17 \pm 10.57
Larynx	D _{mean}	-0.12 \pm 0.14	-0.61 \pm 2.46	-0.69 \pm 2.56	0.45 \pm 0.60	-0.11 \pm 1.82	0.09 \pm 1.24
	D _{50%}	-0.21 \pm 0.25	-0.84 \pm 2.34	-0.98 \pm 2.50	0.18 \pm 0.46	-0.12 \pm 1.68	0.17 \pm 1.45
Mandible	D _{1cc}	0.27 \pm 0.40	0.64 \pm 0.49	0.90 \pm 0.79	-0.73 \pm 1.56	1.44 \pm 1.85	0.52 \pm 0.34
	D _{0.035cc}	0.45 \pm 0.40	0.83 \pm 0.38	1.23 \pm 0.58	0.65 \pm 0.52	1.41 \pm 1.42	1.65 \pm 1.21

ROI — region of interest; CTV — clinical target volume; PTV — planning target volume; SD — standard deviation; ΔD_R — dose variation in rotational error plan; ΔD_T — dose variation in translational error plan; ΔD_{T+R} — dose variation in translational plus rotational error plan

The mean dosimetric impact of the R_{Error} on CTVs, PTVs, and OARs was relatively smaller than the T_{Error} and $T+R_{Error}$. It is attributed to the PTV margin of 5 mm. However, a significant mean dosimetric impact occurred due to T_{Error} and $T+R_{Error}$. The maximum dose variation for the targets and OARs was observed in the $T+R_{Error}$ as the R_{Error} coupled with the T_{Error} could significantly impact the delivered dose. It implies that a smaller R_{Error} coupled with a larger T_{Error} could significantly increase the dose variation. Similar results were reported by Gucken-

berger et al. [24], that the R_{Error} is of clinical significance and is independent of the T_{Error} . Fu et al. [28] reported a substantial decrease in CTV dose for patients with large systematic R_{Error} . Similarly, R_{Error} in larger targets could significantly affect the dose delivery and dose variation.

The single fraction maximum T_{Error} and R_{Error} ranged from 7–8 mm and 2.9⁰–3.0⁰, respectively, which resulted in a significant variation of dose metrics in target volumes and OARs. With no setup error correction, the maximum ΔD (%)

Table 5. The overall mean percentage dose variation in targets and organs at risk (OARs) for 10 intensity-modulated radiation therapy (IMRT) and 10 volumetric modulated arc therapy (VMAT) patients for corresponding dose metrics with moderate setup error correction approach

ROI	Dose-Index	IMRT (n = 10)			VMAT (n = 10)		
		ΔD_R (%) Mean \pm SD	ΔD_T (%) Mean \pm SD	ΔD_{T+R} (%) Mean \pm SD	ΔD_R (%) Mean \pm SD	ΔD_T (%) Mean \pm SD	ΔD_{T+R} (%) Mean \pm SD
CTV-60	D _{98%}	-0.3 \pm 0.1	-0.3 \pm 0.3	-0.5 \pm 0.4	-0.1 \pm 0.1	-0.3 \pm 0.2	-0.4 \pm 0.3
	D _{95%}	-0.1 \pm 0.1	-0.2 \pm 0.2	-0.3 \pm 0.3	0.0 \pm 0.1	-0.3 \pm 0.1	-0.3 \pm 0.2
	D _{2%}	0.1 \pm 0.1	0.3 \pm 0.3	0.4 \pm 0.3	0.1 \pm 0.1	0.1 \pm 0.2	0.2 \pm 0.1
	D _{0.035cc}	0.4 \pm 0.5	0.5 \pm 0.4	0.8 \pm 0.7	0.5 \pm 0.7	0.6 \pm 0.4	1.3 \pm 1.3
CTV-54	D _{98%}	0.0 \pm 0.1	-0.6 \pm 0.6	-0.6 \pm 0.6	-0.3 \pm 0.4	0.1 \pm 0.2	-0.2 \pm 0.3
	D _{95%}	0.0 \pm 0.0	-0.4 \pm 0.4	-0.4 \pm 0.4	-0.3 \pm 0.4	0.1 \pm 0.2	-0.2 \pm 0.4
	D _{2%}	0.2 \pm 0.2	0.6 \pm 0.4	0.8 \pm 0.5	0.4 \pm 0.5	0.4 \pm 0.6	0.8 \pm 0.4
	D _{0.035cc}	0.2 \pm 0.2	1.0 \pm 0.4	1.3 \pm 0.6	0.8 \pm 1.1	0.6 \pm 0.8	1.4 \pm 0.4
PTV-60	D _{98%}	-0.5 \pm 0.4	-3.3 \pm 2.7	-3.7 \pm 2.9	-0.4 \pm 0.3	-2.7 \pm 1.1	-3.1 \pm 1.2
	D _{95%}	-0.3 \pm 0.3	-2.1 \pm 1.9	-2.3 \pm 2.1	-0.2 \pm 0.2	-1.6 \pm 0.8	-1.8 \pm 0.8
	D _{2%}	0.1 \pm 0.1	0.4 \pm 0.3	0.5 \pm 0.3	0.2 \pm 0.1	0.0 \pm 0.0	0.2 \pm 0.1
	D _{0.035cc}	0.6 \pm 0.6	0.9 \pm 1.1	1.3 \pm 1.1	0.7 \pm 0.7	1.3 \pm 0.7	2.1 \pm 1.2
PTV-54	D _{98%}	-0.4 \pm 0.2	-4.5 \pm 3.0	-5.0 \pm 3.0	-0.5 \pm 0.5	-2.4 \pm 1.3	-3.0 \pm 1.5
	D _{95%}	-0.2 \pm 0.1	-2.5 \pm 2.0	-2.7 \pm 2.1	-0.3 \pm 0.4	-1.0 \pm 0.5	-1.3 \pm 0.8
	D _{2%}	0.2 \pm 0.1	0.6 \pm 0.4	0.8 \pm 0.4	0.5 \pm 0.5	0.5 \pm 0.6	0.9 \pm 0.2
	D _{0.035cc}	0.4 \pm 0.4	1.6 \pm 1.3	1.9 \pm 1.3	1.0 \pm 1.3	0.8 \pm 1.7	1.7 \pm 0.9
Spinalcord	D _{1cc}	-0.1 \pm 0.3	-0.1 \pm 1.8	-0.2 \pm 1.9	1.0 \pm 1.4	0.6 \pm 2.4	1.6 \pm 1.5
	D _{0.035cc}	0.1 \pm 0.3	-0.2 \pm 2.0	-0.1 \pm 1.9	0.3 \pm 0.3	2.4 \pm 1.8	2.7 \pm 2.1
Brainstem	D _{1cc}	0.1 \pm 0.5	-1.8 \pm 3.5	-1.7 \pm 3.6	-0.5 \pm 0.5	-0.2 \pm 2.5	-0.7 \pm 3.0
	D _{0.035cc}	-0.1 \pm 0.7	-2.6 \pm 2.3	-2.7 \pm 1.9	-0.7 \pm 0.3	-1.3 \pm 2.7	-2.1 \pm 2.9
L Parotid	D _{mean}	0.9 \pm 0.8	3.4 \pm 6.2	4.3 \pm 6.6	-0.1 \pm 2.4	5.3 \pm 2.4	5.2 \pm 3.2
	D _{50%}	1.6 \pm 2.0	3.7 \pm 13.6	5.7 \pm 15.0	-2.0 \pm 4.1	11.2 \pm 6.7	9.8 \pm 8.9
R Parotid	D _{mean}	-0.1 \pm 0.8	1.3 \pm 9.5	1.2 \pm 10.1	2.3 \pm 2.1	-1.6 \pm 2.0	0.7 \pm 4.2
	D _{50%}	-0.2 \pm 1.9	-0.7 \pm 10.4	-1.3 \pm 11.2	5.8 \pm 5.5	0.2 \pm 4.9	6.0 \pm 10.0
Larynx	D _{mean}	-0.1 \pm 0.1	-0.5 \pm 1.9	-0.6 \pm 2.0	0.2 \pm 0.6	-0.4 \pm 1.4	-0.2 \pm 0.8
	D _{50%}	-0.2 \pm 0.2	-0.7 \pm 1.8	-0.8 \pm 1.9	0.3 \pm 0.3	-0.1 \pm 1.4	0.2 \pm 1.1
Mandible	D _{1cc}	0.2 \pm 0.3	0.4 \pm 0.6	0.5 \pm 0.9	-1.0 \pm 1.5	1.0 \pm 1.9	0.1 \pm 0.6
	D _{0.035cc}	0.3 \pm 0.3	0.5 \pm 0.5	0.8 \pm 0.8	0.1 \pm 0.2	0.6 \pm 1.0	0.8 \pm 1.0

ROI — region of interest; CTV — clinical target volume; PTV — planning target volume; SD — standard deviation; ΔD_R — dose variation in rotational error plan; ΔD_T — dose variation in translational error plan; ΔD_{T+R} — dose variation in translational plus rotational error plan

for D_{98%} in CTV-60, CTV-54, PTV-60, and PTV-54 was -1.2%, -1.9%, -12.0%, and -12.3%, respectively, in the T+R_{Error}. The maximum ΔD (%) for D_{0.035cc} in the spinal cord was 6.5% in the T+R_{Error}. The maximum ΔD (%) for D_{mean} in the left parotid and right parotid was 15.8% and 24.6%, respectively, in the T+R_{Error} (Fig. 4). Similarly, with moderate setup error correction, the maximum ΔD (%) for D_{98%} in CTV-60, CTV-54, PTV-60, and PTV-54 was -1.0%, -1.7%, -9.2%, and -9.5%, respectively, in the T+R_{Error}. The maximum ΔD (%) for

D_{0.035cc} in the spinal cord was 5.4% in the T+R_{Error}. The maximum ΔD (%) for D_{mean} in the left parotid and right parotid was 12.2% and 19.6%, respectively, in the T+R_{Error} (Fig. 5). This study with no setup error correction and moderate setup error correction approaches demonstrated that for patients with substantial setup errors, the uncorrected 6D setup errors have a potential dosimetric impact on the D_{98%} of CTV-60 and CTV-54. However, the mean dosimetric impact for the study patient cohort was not dosimetrically significant.

It is attributed to the uniform PTV margin of 5 mm in the original treatment plan compared to the PTV margins of 4.7 mm, 3.9 mm, and 4.5 mm along the lateral, longitudinal, and vertical axes evaluated for the study patient cohort. For patients with significant setup errors, the uncorrected 6D setup errors have a potential dosimetric impact on the $D_{98\%}$ and $D_{95\%}$ in PTV-60 and PTV-54. The left parotid showed a significant dosimetric impact on D_{mean} in T_{Error} and R_{Error} . For patients with large setup errors, the uncorrected 6D setup errors have a potential dosimetric impact on the $D_{0.035\text{cc}}$ of spinal cord and mandible and the D_{mean} of the left parotid and right parotid. Our study with no setup error correction and moderate setup error correction showed that the uncorrected 6D setup errors result in a significant decrease in the target doses and a non-significant increase in the doses to OARs. It might result in inferior tumor control and increased normal tissue toxicity.

The dosimetric impact of R_{Error} , T_{Error} , and $T+R_{\text{Error}}$ for IMRT (10) and VMAT (10) plans on targets and OARs in ca-tongue patients was evaluated with no correction (Tab. 4) and moderate correction of setup error (Tab. 5). For CTV-60, the dose variation in $D_{98\%}$ and $D_{95\%}$ due to T_{Error} , and $T+R_{\text{Error}}$ in VMAT plans was slightly higher than that in IMRT plans. The dose variation in $D_{98\%}$ and $D_{95\%}$ for IMRT plans was slightly higher than that in VMAT plans for R_{Error} (Tab. 4, 5). However, for PTV-60, the dose variation in $D_{98\%}$ and $D_{95\%}$ due to R_{Error} , T_{Error} , and $T+R_{\text{Error}}$ in IMRT was higher than in VMAT plans (Tab. 4 and 5). For the Spinalcord the dose variation in $D_{1\text{cc}}$ and $D_{0.035\text{cc}}$ due to R_{Error} , T_{Error} , and $T+R_{\text{Error}}$ was higher in VMAT than IMRT plans (Tab. 4, 5). There is no clinically significant difference ($> 2\%$) in dose variation between IMRT and VMAT plans for all targets and OARs except for PTV-54 in $D_{98\%}$ due to T_{Error} and $T+R_{\text{Error}}$ for Spinalcord in $D_{0.035\text{cc}}$ due to T_{Error} and $T+R_{\text{Error}}$ for Braistem in $D_{1\text{cc}}$ due to T_{Error} and $T+R_{\text{Error}}$ for the left parotid in $D_{50\%}$ due to T_{Error} and $T+R_{\text{Error}}$, and for right parotid in D_{mean} and $D_{50\%}$ due to R_{Error} and in $D_{50\%}$ due to $T+R_{\text{Error}}$. This could be due to the comparison of IMRT and VMAT plans for different patients optimized with different priorities for objectives and constraints, and different geometries of targets and OARs. VMAT and IMRT plans could generate similar dose conformity and lower MU with shorter treatment time is

the significant advantage of VMAT over IMRT [44–47]. The true comparison of the dosimetric impact of setup error on IMRT and VMAT plans can be evaluated for IMRT and VMAT plans of the same patients.

The limitation of this study was not considering the dosimetric impact of intrafraction error, which has a considerable impact on delivered doses. However, the magnitude of the dosimetric impact of intrafraction setup errors could be smaller than that of interfraction setup errors. Also, the sole aim of this study was to evaluate the dosimetric impact of 6D interfractional setup errors. The dosimetric evaluation was done on CBCT, which could be affected by a larger patient scatter in CBCT compared to pCT. However, this effect was eliminated by generating the CBCT_REF without R_{Error} and T_{Error} . For dosimetric evaluation, the dose delivered in each fraction was reconstructed on CBCT_REF and compared with the reconstructed doses of R_{Error} , T_{Error} , and $T+R_{\text{Error}}$ on pre-treatment CBCT. The absolute dose variation of the setup error was derived from the original treatment plan by applying the percentage dose variation correction obtained from CBCT plans. It is analogous to the method used by Hatten et al. [36]. The limited FOV and scan length of the CBCT restrict this method to the dosimetric evaluation of small tumor volumes in head and neck patients.

Conclusions

This study demonstrated and assessed the dosimetric impact of uncorrected daily rotational, translational, and 6D translational plus rotational setup errors with no setup error correction and moderate setup error correction approaches, indicating that statistically significant underdosing of target volumes ($p < 0.05$) and significant overdosing of OARs can occur. The substantial magnitude of the maximum dose variation ΔD (%) in PTVs and OARs emphasizes the necessity of accurate daily patient setup verification and target localization with daily correction of interfractional 6D setup errors in modern IMRT and VMAT radiation therapy techniques.

Acknowledgements

Nothing to disclose.

Conflict of interest

The authors have no conflicts of interest to declare that are relevant to the content of this article

Funding

Nothing to disclose.

References

- de Martel C, Plummer M, Vignat J, et al. Worldwide burden of cancer attributable to HPV by site, country and HPV type. *Int J Cancer*. 2017; 141(4): 664–670, doi: [10.1002/ijc.30716](https://doi.org/10.1002/ijc.30716), indexed in Pubmed: [28369882](https://pubmed.ncbi.nlm.nih.gov/28369882/).
- Bortfeld T. IMRT: a review and preview. *Phys Med Biol*. 2006; 51(13): R363–R379, doi: [10.1088/0031-9155/51/13/R21](https://doi.org/10.1088/0031-9155/51/13/R21), indexed in Pubmed: [16790913](https://pubmed.ncbi.nlm.nih.gov/16790913/).
- Otto K. Volumetric modulated arc therapy: IMRT in a single gantry arc. *Med Phys*. 2008; 35(1): 310–317, doi: [10.1118/1.2818738](https://doi.org/10.1118/1.2818738), indexed in Pubmed: [18293586](https://pubmed.ncbi.nlm.nih.gov/18293586/).
- Nutting CM, Morden JP, Harrington KJ, et al. PARSPORT trial management group. Parotid-sparing intensity modulated versus conventional radiotherapy in head and neck cancer (PARSPORT): a phase 3 multicentre randomised controlled trial. *Lancet Oncol*. 2011; 12(2): 127–136, doi: [10.1016/S1470-2045\(10\)70290-4](https://doi.org/10.1016/S1470-2045(10)70290-4), indexed in Pubmed: [21236730](https://pubmed.ncbi.nlm.nih.gov/21236730/).
- Marta GN, Silva V, de Andrade Carvalho H, et al. Intensity-modulated radiation therapy for head and neck cancer: systematic review and meta-analysis. *Radiother Oncol*. 2014; 110(1): 9–15, doi: [10.1016/j.radonc.2013.11.010](https://doi.org/10.1016/j.radonc.2013.11.010), indexed in Pubmed: [24332675](https://pubmed.ncbi.nlm.nih.gov/24332675/).
- Gupta T, Kannan S, Ghosh-Laskar S, et al. Systematic review and meta-analyses of intensity-modulated radiation therapy versus conventional two-dimensional and/or or three-dimensional radiotherapy in curative-intent management of head and neck squamous cell carcinoma. *PLoS One*. 2018; 13(7): e0200137, doi: [10.1371/journal.pone.0200137](https://doi.org/10.1371/journal.pone.0200137), indexed in Pubmed: [29979726](https://pubmed.ncbi.nlm.nih.gov/29979726/).
- Alterio D, Marvaso G, Ferrari A, et al. Modern radiotherapy for head and neck cancer. *Semin Oncol*. 2019; 46(3): 233–245, doi: [10.1053/j.seminoncol.2019.07.002](https://doi.org/10.1053/j.seminoncol.2019.07.002), indexed in Pubmed: [31378376](https://pubmed.ncbi.nlm.nih.gov/31378376/).
- Buciuman N, Marcu LG. Dosimetric justification for the use of volumetric modulated arc therapy in head and neck cancer-A systematic review of the literature. *Laryngoscope Investig Otolaryngol*. 2021; 6(5): 999–1007, doi: [10.1002/lio2.642](https://doi.org/10.1002/lio2.642), indexed in Pubmed: [34667842](https://pubmed.ncbi.nlm.nih.gov/34667842/).
- Jaffray DA. Image-guided radiotherapy: from current concept to future perspectives. *Nat Rev Clin Oncol*. 2012; 9(12): 688–699, doi: [10.1038/nrclinonc.2012.194](https://doi.org/10.1038/nrclinonc.2012.194), indexed in Pubmed: [23165124](https://pubmed.ncbi.nlm.nih.gov/23165124/).
- Boda-Heggemann J, Lohr F, Wenz F, et al. kV cone-beam CT-based IGRT: a clinical review. *Strahlenther Onkol*. 2011; 187(5): 284–291, doi: [10.1007/s00066-011-2236-4](https://doi.org/10.1007/s00066-011-2236-4), indexed in Pubmed: [21533757](https://pubmed.ncbi.nlm.nih.gov/21533757/).
- De Los Santos J, Popple R, Agazaryan N, et al. Image guided radiation therapy (IGRT) technologies for radiation therapy localization and delivery. *Int J Radiat Oncol Biol Phys*. 2013; 87(1): 33–45, doi: [10.1016/j.ijrobp.2013.02.021](https://doi.org/10.1016/j.ijrobp.2013.02.021), indexed in Pubmed: [23664076](https://pubmed.ncbi.nlm.nih.gov/23664076/).
- Kearney M, Coffey M, Leong A. A review of Image Guided Radiation Therapy in head and neck cancer from 2009-201 — Best Practice Recommendations for RTTs in the Clinic. *Tech Innov Patient Support Radiat Oncol*. 2020; 14: 43–50, doi: [10.1016/j.tipsro.2020.02.002](https://doi.org/10.1016/j.tipsro.2020.02.002), indexed in Pubmed: [32566769](https://pubmed.ncbi.nlm.nih.gov/32566769/).
- Lu H, Lin H, Feng G, et al. Interfractional and intrafractional errors assessed by daily cone-beam computed tomography in nasopharyngeal carcinoma treated with intensity-modulated radiation therapy: a prospective study. *J Radiat Res*. 2012; 53(6): 954–960, doi: [10.1093/jrr/rrs041](https://doi.org/10.1093/jrr/rrs041), indexed in Pubmed: [22843373](https://pubmed.ncbi.nlm.nih.gov/22843373/).
- Soni S, Pareek P, Manna S, et al. A dosimetric and radiobiological impact of VMAT and 3DCRT on lumbosacral plexuses, an underestimated organ at risk in cervical cancer patients. *Rep Pract Oncol Radiother*. 2022; 27(4): 624–633, doi: [10.5603/RPOR.a2022.0079](https://doi.org/10.5603/RPOR.a2022.0079), indexed in Pubmed: [36196415](https://pubmed.ncbi.nlm.nih.gov/36196415/).
- Benkhaled S, Koshariuk O, Van Esch A, et al. Characteristics and dosimetric impact of intrafraction motion during peripheral lung cancer stereotactic radiotherapy: is a second midpoint cone beam computed tomography of added value? *Rep Pract Oncol Radiother*. 2022; 27(3): 490–499, doi: [10.5603/RPOR.a2022.0047](https://doi.org/10.5603/RPOR.a2022.0047), indexed in Pubmed: [36186683](https://pubmed.ncbi.nlm.nih.gov/36186683/).
- Katayama H, Takahashi S, Kobata T, et al. Impact of rotational errors of whole pelvis on the dose of prostate-based image-guided radiotherapy to pelvic lymph nodes and small bowel in high-risk prostate cancer. *Rep Pract Oncol Radiother*. 2021; 26(6): 906–914, doi: [10.5603/RPOR.a2021.0107](https://doi.org/10.5603/RPOR.a2021.0107), indexed in Pubmed: [34992862](https://pubmed.ncbi.nlm.nih.gov/34992862/).
- Rudat V, Hammoud M, Pillay Y, et al. Impact of the frequency of online verifications on the patient set-up accuracy and set-up margins. *Radiat Oncol*. 2011; 6: 101, doi: [10.1186/1748-717X-6-101](https://doi.org/10.1186/1748-717X-6-101), indexed in Pubmed: [21864393](https://pubmed.ncbi.nlm.nih.gov/21864393/).
- Oh YK, Baek JG, Kim OB, et al. Assessment of setup uncertainties for various tumor sites when using daily CBCT for more than 2200 VMAT treatments. *J Appl Clin Med Phys*. 2014; 15(2): 4418, doi: [10.1120/jacmp.v15i2.4418](https://doi.org/10.1120/jacmp.v15i2.4418), indexed in Pubmed: [24710431](https://pubmed.ncbi.nlm.nih.gov/24710431/).
- Den RB, Doemer A, Kubicek G, et al. Daily image guidance with cone-beam computed tomography for head-and-neck cancer intensity-modulated radiotherapy: a prospective study. *Int J Radiat Oncol Biol Phys*. 2010; 76(5): 1353–1359, doi: [10.1016/j.ijrobp.2009.03.059](https://doi.org/10.1016/j.ijrobp.2009.03.059), indexed in Pubmed: [19540071](https://pubmed.ncbi.nlm.nih.gov/19540071/).
- Delishaj D, Ursino S, Pasqualetti F, et al. Set-up errors in head and neck cancer treated with IMRT technique assessed by cone-beam computed tomography: a feasible protocol. *Radiat Oncol J*. 2018; 36(1): 54–62, doi: [10.3857/roj.2017.00493](https://doi.org/10.3857/roj.2017.00493), indexed in Pubmed: [29621873](https://pubmed.ncbi.nlm.nih.gov/29621873/).
- Cubillos Mesías M, Boda-Heggemann J, Thoelking J, et al. Quantification and Assessment of Interfraction Setup Errors Based on Cone Beam CT and Determination of Safety Margins for Radiotherapy. *PLoS One*. 2016; 11(3): e0150326, doi: [10.1371/journal.pone.0150326](https://doi.org/10.1371/journal.pone.0150326), indexed in Pubmed: [26930196](https://pubmed.ncbi.nlm.nih.gov/26930196/).
- Hong TS, Tomé WA, Chappell RJ, et al. The impact of daily setup variations on head-and-neck intensity-modulated radiation therapy. *Int J Radiat Oncol Biol Phys*. 2005; 61(3): 779–788, doi: [10.1016/j.ijrobp.2004.07.696](https://doi.org/10.1016/j.ijrobp.2004.07.696), indexed in Pubmed: [15708257](https://pubmed.ncbi.nlm.nih.gov/15708257/).

23. Siebers JV, Keall PJ, Wu Q, et al. Effect of patient setup errors on simultaneously integrated boost head and neck IMRT treatment plans. *Int J Radiat Oncol Biol Phys*. 2005; 63(2): 422–433, doi: [10.1016/j.ijrobp.2005.02.029](https://doi.org/10.1016/j.ijrobp.2005.02.029), indexed in Pubmed: [16168835](https://pubmed.ncbi.nlm.nih.gov/16168835/).
24. Guckenberger M, Meyer J, Vordermark D, et al. Magnitude and clinical relevance of translational and rotational patient setup errors: a cone-beam CT study. *Int J Radiat Oncol Biol Phys*. 2006; 65(3): 934–942, doi: [10.1016/j.ijrobp.2006.02.019](https://doi.org/10.1016/j.ijrobp.2006.02.019), indexed in Pubmed: [16751076](https://pubmed.ncbi.nlm.nih.gov/16751076/).
25. Lawson JD, Elder E, Fox T, et al. Quantification of dosimetric impact of implementation of on-board imaging (OBI) for IMRT treatment of head-and-neck malignancies. *Med Dosim*. 2007; 32(4): 287–294, doi: [10.1016/j.meddos.2007.02.008](https://doi.org/10.1016/j.meddos.2007.02.008), indexed in Pubmed: [17980830](https://pubmed.ncbi.nlm.nih.gov/17980830/).
26. Prabhakar R, Laviraj MA, Hareesh KP, et al. Impact of patient setup error in the treatment of head and neck cancer with intensity modulated radiation therapy. *Phys Med*. 2010; 26(1): 26–33, doi: [10.1016/j.ejmp.2009.05.001](https://doi.org/10.1016/j.ejmp.2009.05.001), indexed in Pubmed: [19576833](https://pubmed.ncbi.nlm.nih.gov/19576833/).
27. Yan M, Lovelock D, Hunt M, et al. Measuring uncertainty in dose delivered to the cochlea due to setup error during external beam treatment of patients with cancer of the head and neck. *Med Phys*. 2013; 40(12): 121724, doi: [10.1118/1.4830427](https://doi.org/10.1118/1.4830427), indexed in Pubmed: [24320510](https://pubmed.ncbi.nlm.nih.gov/24320510/).
28. Fu W, Yang Y, Yue NJ, et al. Dosimetric influences of rotational setup errors on head and neck carcinoma intensity-modulated radiation therapy treatments. *Med Dosim*. 2013; 38(2): 125–132, doi: [10.1016/j.meddos.2012.09.003](https://doi.org/10.1016/j.meddos.2012.09.003), indexed in Pubmed: [23266161](https://pubmed.ncbi.nlm.nih.gov/23266161/).
29. Kaur I, Rawat S, Ahlawat P, et al. Dosimetric impact of setup errors in head and neck cancer patients treated by image-guided radiotherapy. *J Med Phys*. 2016; 41(2): 144–148, doi: [10.4103/0971-6203.181640](https://doi.org/10.4103/0971-6203.181640), indexed in Pubmed: [27217627](https://pubmed.ncbi.nlm.nih.gov/27217627/).
30. Jiang P, Zhang X, Wei S, et al. Set-up error and dosimetric analysis of HexaPOD evo RT 6D couch combined with cone beam CT image-guided intensity-modulated radiotherapy for primary malignant tumor of the cervical spine. *J Appl Clin Med Phys*. 2020; 21(4): 22–30, doi: [10.1002/acm2.12840](https://doi.org/10.1002/acm2.12840), indexed in Pubmed: [32170991](https://pubmed.ncbi.nlm.nih.gov/32170991/).
31. Otsuka M, Monzen H, Ishikawa K, et al. Variations of the Dose Distribution Between CT- and CBCT-based Plans for Oropharyngeal Cancer. *In Vivo*. 2019; 33(4): 1271–1277, doi: [10.21873/invivo.11599](https://doi.org/10.21873/invivo.11599), indexed in Pubmed: [31280218](https://pubmed.ncbi.nlm.nih.gov/31280218/).
32. Lowther NJ, Marsh SH, Louwe RJW. Dose accumulation to assess the validity of treatment plans with reduced margins in radiotherapy of head and neck cancer. *Phys Imaging Radiat Oncol*. 2020; 14: 53–60, doi: [10.1016/j.phro.2020.05.004](https://doi.org/10.1016/j.phro.2020.05.004), indexed in Pubmed: [33458315](https://pubmed.ncbi.nlm.nih.gov/33458315/).
33. Ho KF, Marchant T, Moore C, et al. Monitoring dosimetric impact of weight loss with kilovoltage (kV) cone beam CT (CBCT) during parotid-sparing IMRT and concurrent chemotherapy. *Int J Radiat Oncol Biol Phys*. 2012; 82(3): e375–e382, doi: [10.1016/j.ijrobp.2011.07.004](https://doi.org/10.1016/j.ijrobp.2011.07.004), indexed in Pubmed: [22197229](https://pubmed.ncbi.nlm.nih.gov/22197229/).
34. Noble DJ, Yeap PL, Seah SYK, et al. Anatomical change during radiotherapy for head and neck cancer, and its effect on delivered dose to the spinal cord. *Radiother Oncol*. 2019; 130: 32–38, doi: [10.1016/j.radonc.2018.07.009](https://doi.org/10.1016/j.radonc.2018.07.009), indexed in Pubmed: [30049455](https://pubmed.ncbi.nlm.nih.gov/30049455/).
35. Rong Yi, Smilowitz J, Tewatia D, et al. Dose calculation on kV cone beam CT images: an investigation of the Hu-density conversion stability and dose accuracy using the site-specific calibration. *Med Dosim*. 2010; 35(3): 195–207, doi: [10.1016/j.meddos.2009.06.001](https://doi.org/10.1016/j.meddos.2009.06.001), indexed in Pubmed: [19931031](https://pubmed.ncbi.nlm.nih.gov/19931031/).
36. Hatton J, McCurdy B, Greer PB. Cone beam computerized tomography: the effect of calibration of the Hounsfield unit number to electron density on dose calculation accuracy for adaptive radiation therapy. *Phys Med Biol*. 2009; 54(15): N329–N346, doi: [10.1088/0031-9155/54/15/N01](https://doi.org/10.1088/0031-9155/54/15/N01), indexed in Pubmed: [19590116](https://pubmed.ncbi.nlm.nih.gov/19590116/).
37. Barateau A, Garloiseau C, Cugny A, et al. Dose calculation accuracy of different image value to density tables for cone-beam CT planning in head & neck and pelvic localizations. *Phys Med*. 2015; 31(2): 146–151, doi: [10.1016/j.ejmp.2014.12.007](https://doi.org/10.1016/j.ejmp.2014.12.007), indexed in Pubmed: [25595131](https://pubmed.ncbi.nlm.nih.gov/25595131/).
38. de Smet M, Schuring D, Nijsten S, et al. Accuracy of dose calculations on kV cone beam CT images of lung cancer patients. *Med Phys*. 2016; 43(11): 5934, doi: [10.1118/1.4964455](https://doi.org/10.1118/1.4964455), indexed in Pubmed: [27806611](https://pubmed.ncbi.nlm.nih.gov/27806611/).
39. Barateau A, De Crevoisier R, Largent A, et al. Comparison of CBCT-based dose calculation methods in head and neck cancer radiotherapy: from Hounsfield unit to density calibration curve to deep learning. *Med Phys*. 2020; 47(10): 4683–4693, doi: [10.1002/mp.14387](https://doi.org/10.1002/mp.14387), indexed in Pubmed: [32654160](https://pubmed.ncbi.nlm.nih.gov/32654160/).
40. Tang B, Ma J, Xu J, et al. Feasibility of using calibrated cone-beam computed tomography scans to validate the heart dose in left breast post-mastectomy radiotherapy. *J Int Med Res*. 2020; 48(6): 300060520929168, doi: [10.1177/0300060520929168](https://doi.org/10.1177/0300060520929168), indexed in Pubmed: [32567427](https://pubmed.ncbi.nlm.nih.gov/32567427/).
41. Utena Y, Takatsu J, Sugimoto S, et al. Trajectory log analysis and cone-beam CT-based daily dose calculation to investigate the dosimetric accuracy of intensity-modulated radiotherapy for gynecologic cancer. *J Appl Clin Med Phys*. 2021; 22(2): 108–117, doi: [10.1002/acm2.13163](https://doi.org/10.1002/acm2.13163), indexed in Pubmed: [33426810](https://pubmed.ncbi.nlm.nih.gov/33426810/).
42. Shinde P, Jadhav A, Shankar V, et al. Evaluation of kV-CBCT based 3D dose calculation accuracy and its validation using delivery fluence derived dose metrics in Head and Neck Cancer. *Phys Med*. 2022; 96: 32–45, doi: [10.1016/j.ejmp.2022.02.014](https://doi.org/10.1016/j.ejmp.2022.02.014), indexed in Pubmed: [35217498](https://pubmed.ncbi.nlm.nih.gov/35217498/).
43. van Herk M, Remeijer P, Rasch C, et al. The probability of correct target dosage: dose-population histograms for deriving treatment margins in radiotherapy. *Int J Radiat Oncol Biol Phys*. 2000; 47(4): 1121–1135, doi: [10.1016/s0360-3016\(00\)00518-6](https://doi.org/10.1016/s0360-3016(00)00518-6), indexed in Pubmed: [10863086](https://pubmed.ncbi.nlm.nih.gov/10863086/).
44. Buciuman N, Marcu LG. Dosimetric justification for the use of volumetric modulated arc therapy in head and neck cancer-A systematic review of the literature. *Laryngoscope Investig Otolaryngol*. 2021; 6(5): 999–1007, doi: [10.1002/lio2.642](https://doi.org/10.1002/lio2.642), indexed in Pubmed: [34667842](https://pubmed.ncbi.nlm.nih.gov/34667842/).
45. Liu P, Liu G, Wang G, et al. Comparison of Dosimetric Gains Provided by Intensity-Modulated Radiotherapy, Volume-Modulated Arc Therapy, and Helical Tomotherapy for High-Grade Glioma. *Biomed Res Int*. 2020; 2020: 4258989, doi: [10.1155/2020/4258989](https://doi.org/10.1155/2020/4258989), indexed in Pubmed: [32258121](https://pubmed.ncbi.nlm.nih.gov/32258121/).
46. Pigorsch SU, Kampfer S, Oechsner M, et al. Report on planning comparison of VMAT, IMRT and helical tomother-

- apy for the ESCALOX-trial pre-study. *Radiat Oncol.* 2020; 15(1): 253, doi: [10.1186/s13014-020-01693-2](https://doi.org/10.1186/s13014-020-01693-2), indexed in Pubmed: [33138837](https://pubmed.ncbi.nlm.nih.gov/33138837/).
47. Guy JB, Falk AT, Auberdiac P, et al. Dosimetric study of volumetric arc modulation with RapidArc and intensity-modulated radiotherapy in patients with cervical cancer and comparison with 3-dimensional conformal technique for definitive radiotherapy in patients with cervical cancer. *Med Dosim.* 2016; 41(1): 9–14, doi: [10.1016/j.meddos.2015.06.002](https://doi.org/10.1016/j.meddos.2015.06.002), indexed in Pubmed: [26212351](https://pubmed.ncbi.nlm.nih.gov/26212351/).